WASP and SCAR have distinct roles in activating the Arp2/3 complex during myoblast fusion

Susanne Berger[1,*], Gritt Schäfer[1,*], Dörthe A. Kesper[1,‡], Anne Holz[2], Therese Eriksson[3], Ruth H. Palmer[3], Lothar Beck[4], Christian Klämbt[5], Renate Renkawitz-Pohl[1] and Susanne-Filiz Önel[1,§]

[1]Fachbereich Biologie, Entwicklungsbiologie, Philipps-Universität Marburg, Karl-von-Frisch Str. 8, D-35043 Marburg, Germany
[2]Institut für Allgemeine und Spezielle Zoologie, Stephanstr. 24, Justus-Liebig-Universität Giessen, D-35390 Giessen, Germany
[3]UCMP, Umeå University, Building 6L, 90187 Umeå, Sweden
[4]Fachbereich Biologie, Spezielle Zoologie, Philipps-Universität Marburg, Karl-von-Frisch Str. 8, D-35043 Marburg, Germany
[5]Institut für Neurobiologie, Westfälische Wilhelms-Universität Münster, Badestr. 9, D-48149 Münster, Germany

*These authors contributed equally to this work
‡Present address: Abteilung für Entwicklungsbiologie I, Zentrum für Medizinische Biotechnologie, Universität Duisburg-Essen, Universitätsstr., D-45117 Essen, Germany
§Author for correspondence (e-mail: oenel@staff.uni-marburg.de)

Accepted 21 January 2008
Journal of Cell Science 121, 1303-1313 Published by The Company of Biologists 2008
doi:10.1242/jcs.022269

Summary

Myoblast fusion takes place in two steps in mammals and in *Drosophila*. First, founder cells (FCs) and fusion-competent myoblasts (FCMs) fuse to form a trinucleated precursor, which then recruits further FCMs. This process depends on the formation of the fusion-restricted myogenic-adhesive structure (FuRMAS), which contains filamentous actin (F-actin) plugs at the sites of cell contact. Fusion relies on the HEM2 (NAP1) homolog Kette, as well as Blow and WASP, a member of the Wiskott-Aldrich-syndrome protein family. Here, we show the identification and characterization of *schwächling* – a new *Arp3*-null allele. Ultrastructural analyses demonstrate that *Arp3*^{schwächling} mutants can form a fusion pore, but fail to integrate the fusing FCM. Double-mutant experiments revealed that fusion is blocked completely in *Arp3* and *wasp* double mutants, suggesting the involvement of a further F-actin regulator. Indeed, double-mutant analyses with *scar*/*WAVE* and with the WASP-interacting partner *vrp1* (*sltr*, *wip*)/*WIP* show that the F-actin regulator *scar* also controls F-actin formation during myoblast fusion. Furthermore, the synergistic phenotype observed in *Arp3 wasp* and in *scar vrp1* double mutants suggests that WASP and SCAR have distinct roles in controlling F-actin formation. From these findings we derived a new model for actin regulation during myoblast fusion.

Key words: *Drosophila*, Myogenesis, F-actin, *Arp3*, FuRMAS, Actin cytoskeleton, *kette*

Introduction

Intercellular fusion of myoblasts is a crucial process for somatic muscle formation during embryogenesis of *Drosophila* and vertebrates, including mammals (Taylor, 2006). Additionally, in vertebrates, muscle growth after birth requires continuous fusion of myoblasts arising from satellite cells, the stem cells of vertebrate muscles. The somatic musculature of *Drosophila melanogaster* is well-characterized and can serve as a model in which to study and unravel the underlying molecular mechanisms involved in myoblast fusion.

In *Drosophila*, myoblast fusion results from a dynamic relationship between founder cells (FCs) and fusion-competent myoblasts (FCMs) (Bate, 1990). The FCs seed the fusion process and are thus responsible for the unique identity of each muscle fiber. The larger population of FCMs migrate towards, recognize and adhere to the FCs (for reviews, see Abmayr et al., 2005; Baylies et al., 1998; Chen and Olson, 2004; Taylor, 2000). Following these cellular interaction steps, an FC then fuses with one or two FCMs, giving rise to a precursor cell, which in turn merges with additional myoblasts in a second fusion step until the appropriate muscle size is reached (Bate, 1990; Rau et al., 2001). Studies on mammalian cell cultures have revealed that there are strong parallels to this model in vertebrates at the molecular level (Horsley and Pavlath, 2004).

Recently, several essential molecules required for the fusion of FCs and FCMs have been reported. For example, during cell adhesion, membrane-spanning Immunoglobulin (Ig)-molecules are involved in establishing a ring-shaped fusion-restricted myogenic-adhesive structure (FuRMAS) (Kesper et al., 2007). The Ig-domain molecule Dumbfounded [Duf, also known as Kin of Irre (Kirre) (see FlyBase)] (Ruiz-Gomez et al., 2000; Strünkelnberg et al., 2001) forms the ring at cell-contact points in FCs, whereas the Ig-domain protein Sticks and Stones (Sns) (Bour et al., 2000) forms a corresponding structure in FCMs. Both proteins interact heterotypically to initiate the process of myoblast fusion. The progress of fusion is manifested in the expansion of the FuRMAS at the contact sites between FCs and FCMs from 1 μm to 5 μm (Kesper et al., 2007). Interestingly, the Ig-domain protein Duf was recently identified in zebrafish, suggesting a conserved molecular pathway in insects and vertebrates (Srinivas et al., 2007).

Other known components of the FuRMAS include the adaptor protein Rolling pebbles7 [Rols7, also known as Antisocial (Ants)] (Chen and Olson, 2001; Menon and Chia, 2001; Rau et al., 2001) in FCs and Blown fuse (Blow) (Doberstein et al., 1997; Schröter et al., 2006) in FCMs. Rols7 induces the second fusion step (Rau et al., 2001) and is expressed as a ring in FCs, similar to Duf, and delivers the signal from the FC membrane into the cytosol by interacting with the intracellular domain of Duf via its tetratricopeptide (TPR) repeats (Kreisköther et al., 2006). Blow, by contrast, is concentrated as a plug in the center of the ring formed by Sns (Kesper et al., 2007).

During the fusion process, the actin cytoskeleton of myoblasts is dynamically organized. Consistent with this, the center of the adhesion ring in FCs and FCMs contains filamentous actin (F-actin) (Kesper et al., 2007). Recently, we reported that the actin regulators *kette* (Schröter et al., 2004) and *wasp* (Schäfer et al., 2007) are essential for myoblast fusion. Kette is the *Drosophila* homolog of HEM2 (NAP1), and can be found in a complex with SCAR (homolog of the mammalian WAVE) and is a member of the Wiskott-Aldrich-syndrome protein (WASP) family (reviewed by Ibarra et al., 2005). Moreover, *kette* was shown to interact genetically with *blow* during myoblast fusion (Schröter et al., 2004). WASP family members possess a conserved VCA (verprolin homologous, cofilin homologous and acidic) domain, which is involved in the binding of G-actin and Arp2/3 (Rohatgi et al., 1999; Miki and Takenawa, 1998; Machesky et al., 1999). The $wasp^{3D3\text{-}035}$ allele lacks the CA domain of the VCA domain and thus neutralizes the function of maternal WASP (Schäfer et al., 2007). Furthermore, genetic data indicate that Kette antagonizes the function of WASP (Schäfer et al., 2007). The WASP-interacting partner Verprolin1 [Vrp1, also known as Solitary (Sltr) and Wip; the *Drosophila* homolog of the mammalian WIP], however, acts in a complex with WASP to ensure successful myoblast fusion (Kim et al., 2007; Massarwa et al., 2007).

The branching of F-actin is initiated by the de novo nucleation of actin, triggered through the activity of the Arp2/3 complex (reviewed by Takenawa and Miki, 2001). Alone, the Arp2/3 complex is inactive and requires a set of binding partners, including members of the WASP family, to become active (Machesky and Insall, 1998). The binding of these proteins has been proposed to lead to a conformational change in the position of the seven subunits of the Arp2/3 complex, especially in the relative position of the subunits Arp2 and Arp3 (Robinson et al., 2001; Volkmann et al., 2001).

Here, we describe for the first time an EMS-induced *Arp3*-null allele, $Arp3^{schwächling}$, having an abnormal myoblast-fusion phenotype. Ultrastructural analysis of $Arp3^{schwächling}$ and $wasp^{3D3\text{-}035}$ revealed the formation of a fusion pore in both mutants. Whereas in $Arp3^{schwächling}$ mutants the membrane between fusing myoblasts is removed, in $wasp^{3D3\text{-}035}$ embryos, membrane breakdown is not completed. The finding that fusion in $Arp3^{schwächling}$ embryos is disrupted despite the formation of a fusion pore indicates that the pore does not expand in $Arp3^{schwächling}$ mutants. Therefore, to gain a deeper insight into the F-actin regulation of myoblast fusion, we examined *Arp3 wasp* double-mutant embryos, which show a complete block of myoblast fusion. This phenotype suggests that WASP is not the only actin regulator controlling F-actin polymerization during fusion. Indeed, our studies on *scar* single mutants and *scar vrp1* double mutants strongly imply that the first and the second fusion steps require a different set of F-actin nucleation factors.

Results

schwächling is a new *Arp3* allele

The fusion mutant *schwächling* was detected in the same mutagenesis collection in which we previously identified *kette* and *wasp* (Schröter et al., 2004; Schäfer et al., 2007). Upon analysis of the muscle pattern of the ethyl methane sulphonate (EMS)-induced *pointed* allele $pnt^{3D2\text{-}26}$ with the anti-β3-tubulin antibody, we observed an arrest in myoblast fusion. To address whether the mutation in *pnt* is responsible for the fusion defect, we examined the embryonic muscle pattern of the loss-of-function mutant $pnt^{\Delta 88}$. However, *pnt*-null mutants did not show a myoblast-fusion phenotype (data not shown), indicating that the mutation in *pnt* is not responsible for the observed phenotype. Therefore, it is highly likely that the fusion phenotype is caused by a further mutation on the $pnt^{3D2\text{-}26}$-containing chromosome. Complementation tests demonstrated that the additional mutation was not allelic to known mutations in genes required for myoblast fusion, thereby revealing a new fusion-relevant component, which we have named *schwächling*. To characterize the *schwächling* mutant phenotype in detail, we separated the *pnt* locus from the *schwächling* mutation by using meiotic recombination. Homozygous *schwächling* mutants display a severe defect in myoblast fusion (Fig. 1B, arrow).

To map the region in which *schwächling* is localized, we used the deficiency kit for the third chromosome. The deficiency Df(3L)ZP1 was allelic to *schwächling*, and both homozygous (Fig. 1C, arrow) and transheterozygous (Fig. 1D, arrow) embryos had a myoblast-fusion defect. Df(3L)ZP1 is a large deficiency (66A17-66C5) resulting in the removal of approximately 90 open reading frames (ORFs). We also found that the deficiency Df(3L)pbl-X1 (65F3-66B10) is allelic to *schwächling*. To further narrow-down this region, we employed P-element insertions and performed complementation tests. The lethality-causing EP-element insertion $Arp66B^{EP3640}$ did not complement *schwächling*. Moreover, the EP insertion $Arp66B^{EP3640}$ was mapped to the cytological position 66B6 and was found to be inserted in the 5′UTR of the *Drosophila* homolog of the *Arp3* gene *Arp66B* (FlyBase). We observed that homozygous $Arp66B^{EP3640}$ mutant embryos do not exhibit a strong myoblast-fusion defect (Fig. 1E); however, in transheterozygous $Arp66B^{EP3640}$/*schwächling* embryos, a disruption in myoblast fusion was clearly visible (Fig. 1F, arrow). These observations suggest that *schwächling* is a new allele of *Arp3*; we named this allele $Arp3^{schwächling}$. Further support for this finding also comes from RNA in situ hybridizations, which show that the *Arp3* transcript is expressed from stage 10 onwards in the mesoderm (Fig. 1G,H).

Molecular characterization of $Arp3^{schwächling}$

To investigate the molecular basis of the EMS mutation in $Arp3^{schwächling}$, we determined the sequence of *Arp3* in $Arp3^{schwächling}$ homozygous-mutant embryos. Fig. 1J shows the gene structure of *Arp3*. In $Arp3^{schwächling}$ embryos, the *Arp3* gene contains a G→A nucleotide transition at the splice acceptor site of the first intron (Fig. 1J). This point mutation possibly leads to an aberrantly spliced transcript, retaining the first intron, that becomes translated into a truncated protein of 15 amino acids (aa) and can be thus considered as a null allele. To test this notion, RNA was isolated from wild-type, $Arp3^{schwächling}$ heterozygous and homozygous embryos, and used as template in reverse transcriptase-PCR (RT-PCR) assays. We amplified a 509-bp fragment representing the spliced mRNA form of exons 1 and 3 (Fig. 1I, lower arrowhead). In $Arp3^{schwächling}$ heterozygous and homozygous embryos, we additionally obtained a 674-bp product containing the first intron (Fig. 1I, upper arrowhead). However, because this product was present in low amounts, it is highly likely that the spliced form of the product was still present, probably because of the maternal contribution of *Arp3* mRNA.

Fusion in $Arp3^{schwächling}$ is disrupted after precursor formation

Further analysis revealed that the determination of FCs and FCMs in $Arp3^{schwächling}$ mutant embryos occurs normally (data not shown). Consequently, the phenotype in $Arp3^{schwächling}$ embryos is due to a failure of myoblasts to fuse. Myoblast fusion in vertebrates and

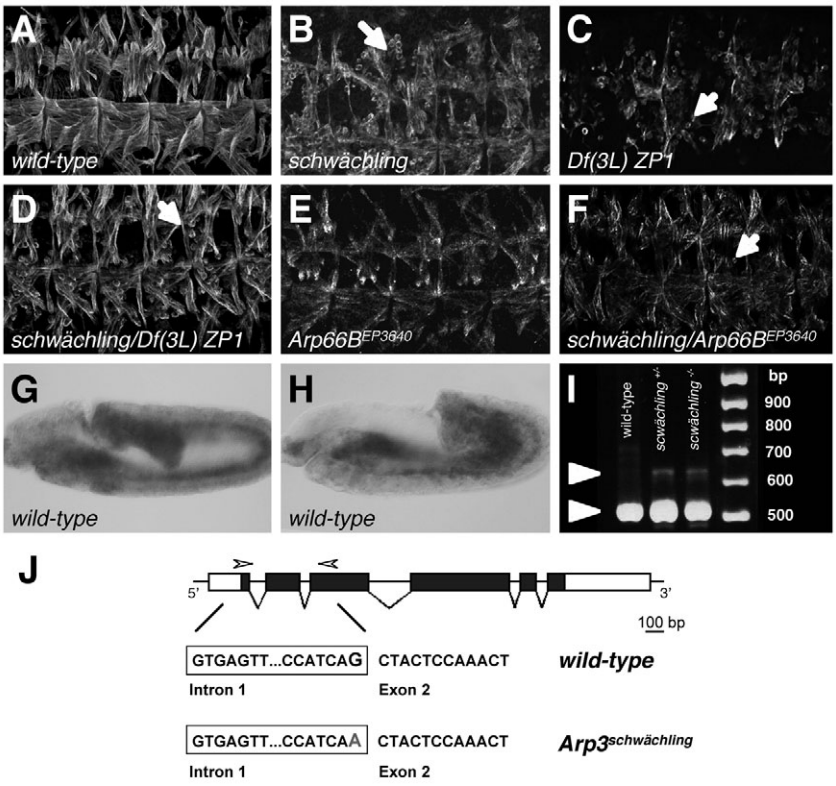

Fig. 1. *schwächling* is a new allele of *Arp3*. (A-F) Embryonic muscle pattern of stage-16 embryos stained with anti-β3-tubulin. (A) Wild-type. (B) Unfused myoblasts are attaching to growing myotubes in *schwächling* homozygous-mutant embryos (arrow). (C,D) The deficiency Df(3L)ZP1 shows a similar phenotype to *schwächling* (C) and also displays an unfused-myoblast phenotype in transheterogeneity to *schwächling* (D). (E,F) The EP-element insertion Arp66B^{EP3640} (E) only displays a fusion defect in embryos that are transheterozygous to *schwächling* (F, arrow). (G,H) In situ hybridizations with a labeled *Arp3* antisense probe show that the *Arp3* transcript is expressed in the mesoderm in stage 10 (G) and late stage 11 (H). (I) RT-PCR on RNA isolated from wild-type, *Arp3*$^{schwächling-/+}$ and *Arp3*$^{schwächling-/-}$ embryos. Spliced *Arp3* mRNA is present in all three lanes (509-bp product). The zygotically transcribed mRNA in *Arp3*$^{schwächling-/+}$ and *Arp3*$^{schwächling-/-}$ embryos is unspliced (674 bp). (J) Schematic drawing of the *Arp3* transcript. The ORF is denoted with shaded boxes. The donor/acceptor splice-site nucleotide sequence of intron 1 from wild-type embryos and *Arp3*^{schwächling} mutant embryos is shown. *schwächling* mutants show a G-to-A transition in the acceptor splice site.

Drosophila proceeds in two distinct steps (Bate, 1990; Beckett and Baylies, 2007; Horsley and Pavlath, 2004; Rau et al., 2001). During the first step, a bi- to tri-nucleated precursor cell forms, which undergoes additional rounds of fusion until the final size of the mature myofiber is reached. The transcription factor Even skipped (Eve) marks the 14 nuclei of the segmentally repeated dorsal muscle DA1 as well as the pericardial cells. To estimate at which stage of fusion *Arp3*^{schwächling} mutant embryos are arrested, we counted the

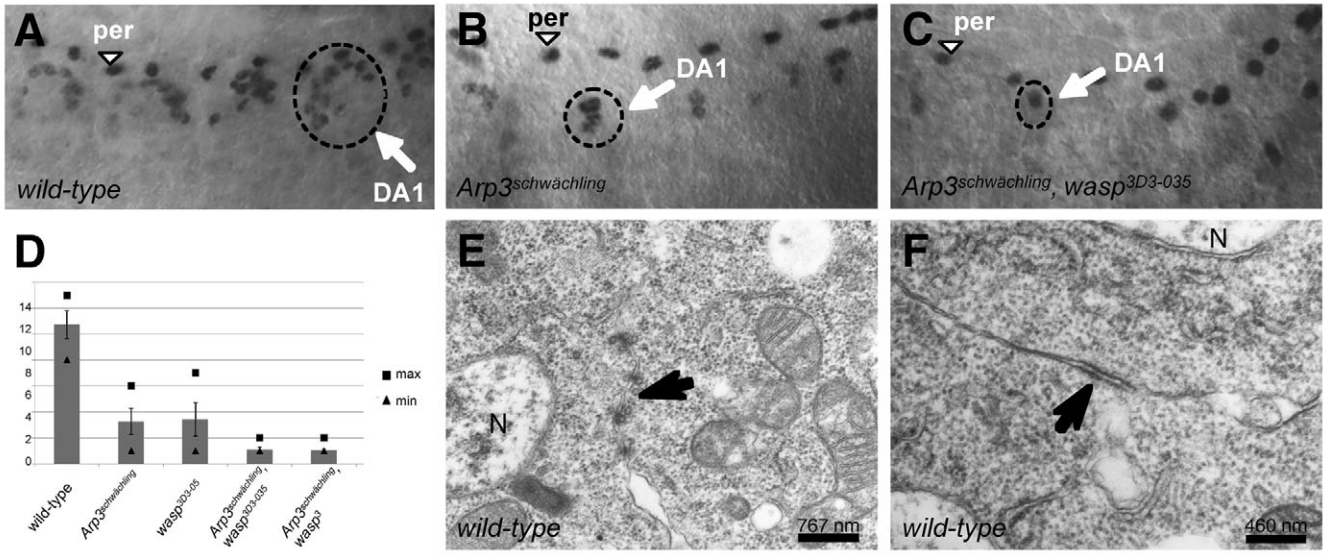

Fig. 2. *Arp3*^{schwächling} mutants stop myoblast fusion after precursor formation. (A-C) Anti-Eve stainings on stage-15 embryos visualize the nuclei of the DA1 muscle (arrow) and the pericardial cells (per). (A) The wild-type DA1 muscle contains up to 14 nuclei. (B) Since fusion is disturbed in homozygous *Arp3*^{schwächling} mutant embryos, the DA1 muscle only contains approximately three nuclei. (C) The DA1 muscle in *Arp3*^{schwächling} *wasp*$^{3D3-035}$ double mutants is mainly mono-nucleated, showing that myoblasts fail to fuse completely. (D) Statistical analysis of the DA1 nuclei confirms that *Arp3*^{schwächling} and *wasp*$^{3D3-035}$ single mutants stop fusion after precursor formation. However, in *Arp3*^{schwächling} *wasp*^{3} double mutants, no fusion takes place. (E,F) Electron microscopy studies on stage-14 wild-type embryos. (E) Assembly of the pre-fusion complex (arrow); (F) arrow marks the electron-dense plaque that is formed between two fusing myoblasts. N, cell nucleus. Magnifications: (E) 12,000×; (F) 21,000×.

nuclei of the DA1 muscle marked by anti-Eve (Fig. 2B,D). The DA1 muscles in *Arp3*^{schwächling} embryos were found to contain, on average, three nuclei, indicating that the first fusion step, forming a bi- to trinucleated precursor cell, had completed.

Ultrastructural analysis of *Arp3*^{schwächling} and *wasp*$^{3D3-035}$ mutant embryos

Arp3 is an actin-related protein that is one of the seven proteins forming the Arp2/3 complex, which is involved in creating new branching actin filaments. The activation of the Arp2/3 complex requires the binding of the WASP family members. In *Drosophila*, there are two members of this family – WASP and SCAR. Both proteins share a common C-terminal Verprolin homologous (V), Cofilin homologous (C) and acidic (A) domain (also known as the VCA domain). The V domain binds monomeric G-actin and the CA domain binds the Arp2/3 complex (Machesky and Insall, 1998; Miki and Takenawa, 1998; Rohatgi et al., 1999). Previously, we reported that the lack of the CA and A domain of WASP blocks myoblast fusion after precursor formation (Schäfer et al., 2007). Thus, in both *Arp3*^{schwächling} and *wasp*$^{3D3-035}$ mutants, myoblasts complete the first fusion step, but fail to undergo the second one.

The second fusion step takes place as several distinct steps that can be distinguished at the ultrastructural level (Doberstein et al., 1997; Schröter et al., 2004). First, electron-dense vesicles appear on adjacent myoblast membranes. This structure is known as the pre-fusion complex (Fig. 2E, arrow). The vesicles are thought to disintegrate and give rise to the so-called electron-dense plaques (Fig. 2F, arrow). At the contact area between a precursor cell and an FCM (Fig. 3A,A′, between the arrows), membranes start to vesiculate, initiating the breakdown of the membrane (Fig. 3A′, arrowheads).

In ultrathin sections of *Arp3*^{schwächling} embryos, we observed the formation of a fusion pore between a growing myotube and an FCM (Fig. 3C, overview; Fig.3C′, arrows). However, we did not observe any plasma membrane remnants between the cells, as seen in wild-type embryos (Fig. 3A′, next to the arrowheads). We therefore conclude that *Arp3*^{schwächling} embryos stop fusion after membrane breakdown, when a fusion pore has been formed. By contrast, ultrathin sections of *wasp*$^{3D3-035}$ embryos revealed that membrane breakdown fails to complete in these mutants (Fig. 3B; Fig. 3B′, between arrowheads). Hence, *wasp* is required for the creation of a fusion pore, whereas *Arp3* is required to integrate FCMs into the growing myotube after fusion-pore formation.

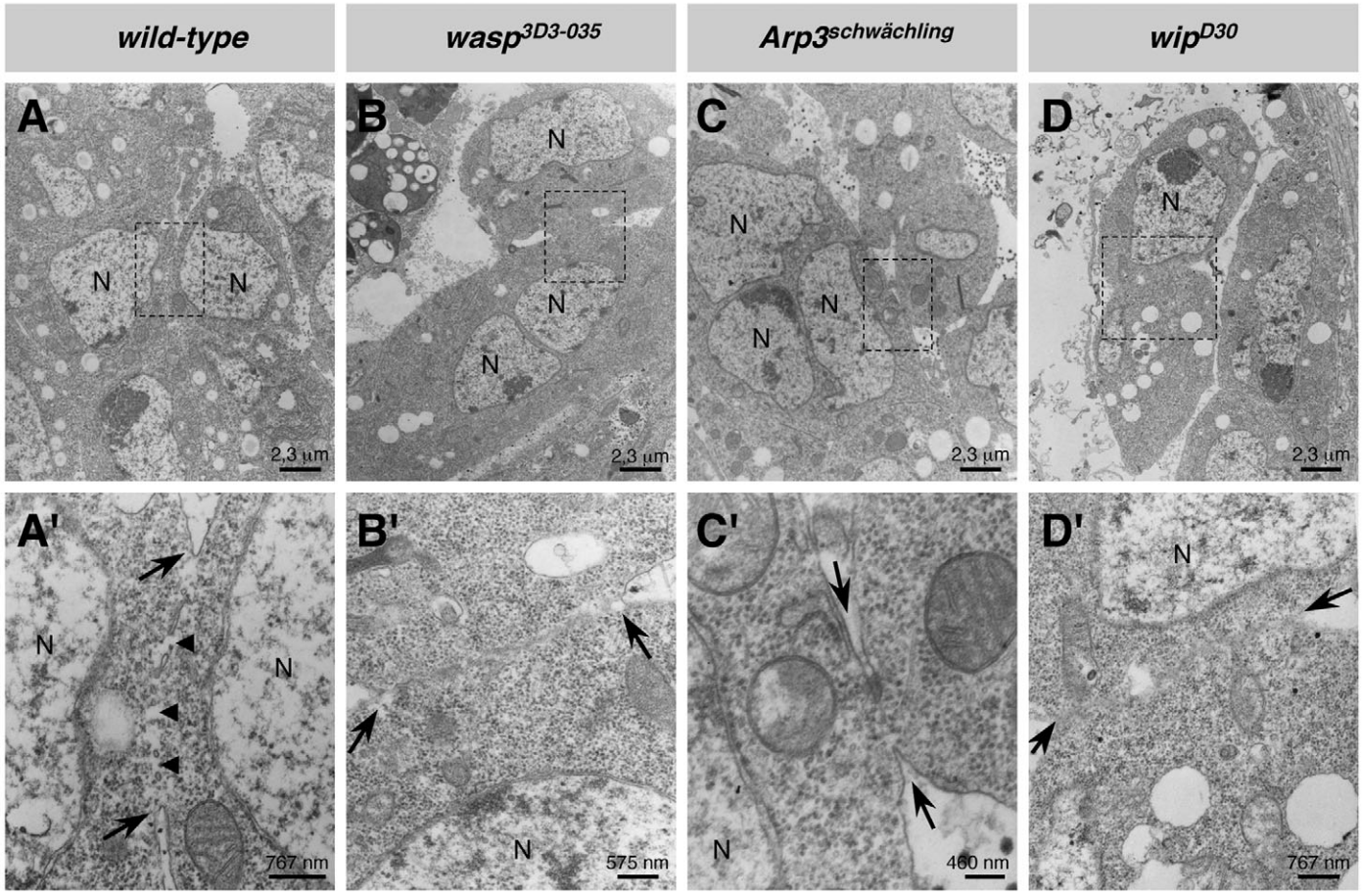

Fig. 3. *wasp*$^{3D3-035}$ and *wip*^{D30} single mutants stop fusion during fusion-pore formation, whereas, in *Arp3*^{schwächling} mutants, a fusion pore is formed. (A-D) Ultrathin sections of stage-14 embryos show myoblasts in the process of fusion (boxed area). (A′-D′) Higher-magnification views of the boxed areas. (A,A′) Wild type. (A′) A forming fusion pore (arrows) and vesiculating membranes (arrowheads). (B) Myoblast fusing to a precursor cell in a *wasp*$^{3D3-035}$ embryo. (B′) The higher-magnification view shows that membranes are vesiculating. (C) In *Arp*^{schwächling} mutant embryos, a trinucleated precursor cell is surrounded by several myoblasts. (C′) A fusion pore has formed between the precursor cell and the FCM, but the FCM fails to integrate into the muscle. (D) Fusing myoblasts in a *wip*^{D30} (*vrp1*) embryo. (D′) Vesiculating membranes. N, cell nucleus. Magnification: (A-D) 3600×; (A′,D′) 12,000×; (B′,C′) 21,000×.

Recently, two papers have described the identification of a WASP-interacting partner named Vrp1 as an essential component for myoblast fusion (Kim et al., 2007; Massarwa et al., 2007). To date, two *vrp1* alleles, namely *wip*^{D30} and *sltr*^{S1946}, are known to stop fusion after precursor formation. Because we observed that *wasp*$^{3D3\text{-}035}$ mutants arrest fusion during membrane removal, but that a very different phenotype for *vrp1* has recently been reported (Kim et al., 2007), we reinvestigated the phenotype of *vrp1* mutant embryos by electron microscopy. For this purpose, we used the characterized *wip*^{D30} allele. Our analysis confirmed that *wip*^{D30} mutants (Fig. 3D,D′) are arrested during membrane breakdown – a finding also reported by Massarwa et al. (Massarwa et al., 2007) – and that this arrested stage is the same as found in *wasp*$^{3D3\text{-}035}$ mutants (Fig. 3B,B′).

WASP is not the only essential activator of the Arp2/3 complex in myoblast fusion

To gain further insight into the relevance of F-actin regulation during myoblast fusion, we generated and investigated *Arp3*^{schwächling} and *wasp*$^{3D3\text{-}035}$ double-mutant embryos. As described previously, the *wasp* allele *wasp*$^{3D3\text{-}035}$ carries a point mutation that leads to loss of the CA domain of the VCA module (Schäfer et al., 2007). *wasp*$^{3D3\text{-}035}$ mutants show an unfused myoblast phenotype (Fig. 4B,B′). Because the CA domain is essential for binding of the Arp2/3 complex, we predicted that the phenotype of the double mutants would resemble that of *wasp*$^{3D3\text{-}035}$ mutant embryos. Instead, we observed a strongly enhanced myoblast-fusion phenotype (Fig. 4C,C′). To analyze the *Arp3*^{schwächling} *wasp*$^{3D3\text{-}035}$ mutant phenotype more precisely, we examined the DA1 muscle with the nuclear marker anti-Eve. The DA1 muscle was found to only contain one nucleus per hemisegment (Fig. 2C,D), indicating that fusion is blocked completely in the double mutant. To examine the interaction of *Arp3* and *wasp* during myoblast fusion more closely, we performed the double-mutant analysis with weaker alleles of *Arp3* and *wasp*. This analysis revealed that, in *Arp3*^{schwächling} *wasp*^{3} and *Arp66B*^{EP3640} *wasp*$^{3D3\text{-}035}$ double mutants, fusion is also blocked completely (data not shown). *wasp* and *Arp3* mRNA are maternally contributed. In the case of *wasp*, maternal *wasp* is sufficient to complete myoblast fusion (Schäfer et al., 2007). We therefore expected that fusion would not be blocked completely, but that the first fusion step, but possibly not the second, would take place in *wasp Arp3* double-mutant embryos. The enhanced fusion defect observed in the double mutant led us to propose that *wasp* is only required during the second fusion step. As a consequence, a different Arp2/3 activator besides WASP must regulate the activity of the Arp2/3 complex during the first step of myoblast fusion.

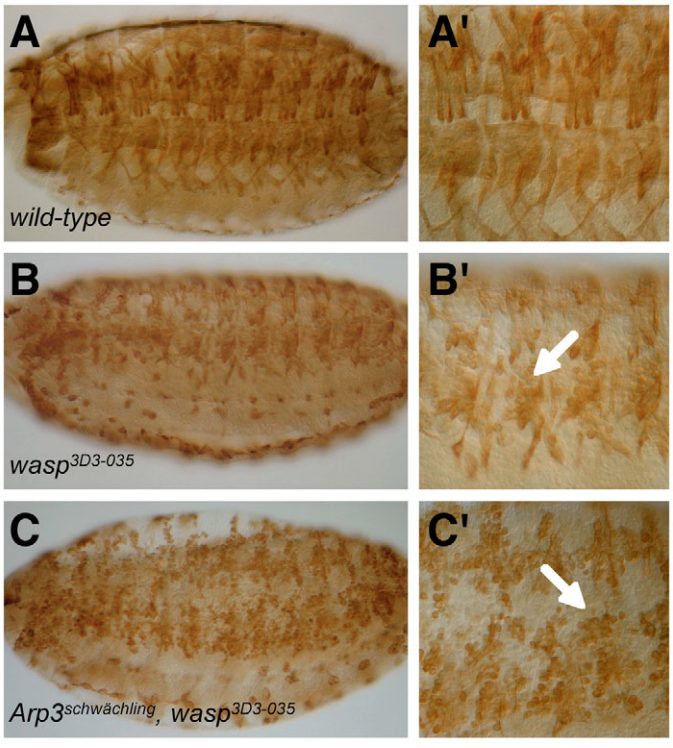

Fig. 4. Fusion is blocked in *Arp3*^{schwächling} *wasp*$^{3D3\text{-}035}$ double mutants. (A-C) Visualization of the somatic musculature of stage-16 embryos by staining for anti-β3-tubulin. (A′-C′) Higher-magnification views. (A,A′) Wild type. (B,B′) *wasp*$^{3D3\text{-}035}$ mutant embryo with unfused myoblasts. (C,C′) The unfused-myoblast phenotype of the single mutants *Arp3*^{schwächling} (see Fig. 1B) and *wasp*$^{3D3\text{-}035}$ is enhanced in homozygous *Arp3*^{schwächling} *wasp*$^{3D3\text{-}035}$ double mutants (C′, arrow).

In addition to the WASP-Vrp1 complex, SCAR also controls Arp2/3-regulated F-actin formation during myoblast fusion

The activity of the Arp2/3 complex is regulated by nucleation-promoting factors such as WASP and SCAR. To determine whether *scar* is required for myoblast fusion, we examined a hypomorphic and a null allele of *Drosophila scar*, and generated double mutants with *scar* and components of the WASP complex.

First we examined the muscle pattern of homozygous *scar*^{k13811} and *scar*$^{\Delta 37}$ mutants (Zallen et al., 2002) using the anti-β3-tubulin antibody. We observed a weak fusion defect in these embryos. The unfused myoblast phenotype in homozygous *scar*$^{\Delta 37}$ embryos was more severe than in homozygous *scar*^{k13811} mutants (Fig. 5). Nevertheless, unfused myoblasts were visible in both *scar* mutants and muscles seemed to be reduced in size in *scar*$^{\Delta 37}$ mutants (Fig. 5E, arrowhead). We further noticed that dorsal closure is incomplete in both *scar* mutants. Similar to *wasp* and *Arp3* mRNA, *scar* mRNA is maternally contributed (Zallen et al., 2002). This might explain why *scar*-null mutants still show considerable myoblast fusion. To investigate whether *scar* and *wasp* interact genetically during myoblast fusion, we performed a dosis experiment and generated *scar wasp* double mutants. We used the *scar*^{k13811} and *wasp*^{3} alleles, which display only a very weak myoblast-fusion phenotype, for this experiment. Taking out one copy of *wasp*^{3} in a *scar*^{k13811} mutant background intensified the appearance of unfused myoblasts (Fig. 5B, arrow). This phenotype became even more severe in *scar*^{k13811} *wasp*^{3} double-mutant embryos (Fig. 5C, arrow). These findings support our notion that myoblast fusion in *Drosophila* is regulated via both members of the WASP family. WASP and its interacting partner Vrp1 are both essential for myoblast fusion. Thus, we next examined whether *scar* and *vrp1* also interact genetically.

In addition to the known *vrp1* alleles, there is a piggyBac insertion from the Harvard *Drosophila* stock collection available named *vrp1*^{f06715}. We found that *vrp1*^{f06715} does not complement the deficiencies Df(2R)Exel6078 and Df(2R)Exel7010, and is allelic to *wip*^{D30}. Fig. 5F shows that some fusion takes place in *vrp1*^{f06715} embryos; however, at the end of embryogenesis the growing myotubes are still surrounded by numerous unfused myoblasts. This phenotype is similar to the one observed in *wip*^{D30} mutants. To assess the role of the WASP-Vrp1 complex and SCAR during myoblast fusion, we generated *scar*$^{\Delta 37}$ *vrp1*^{f06715} double mutants.

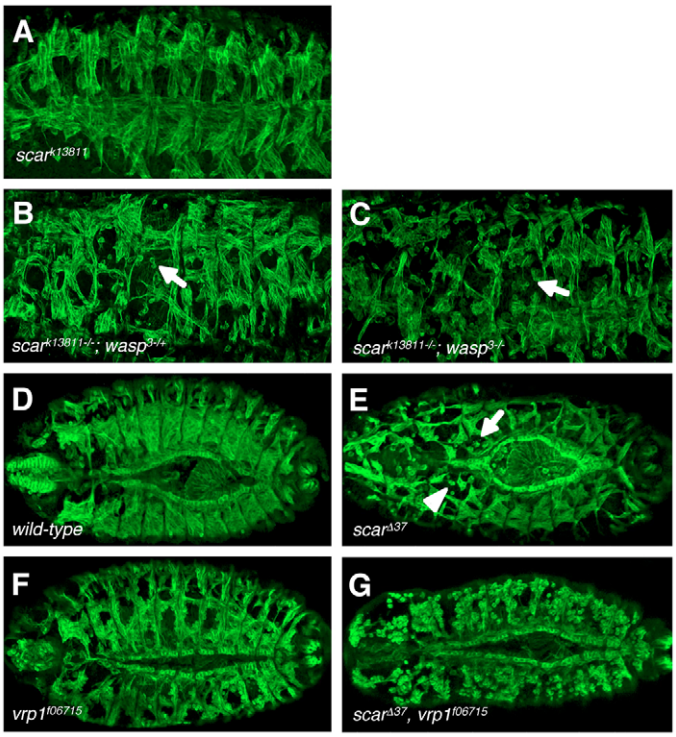

Fig. 5. The Arp2/3 regulators SCAR and the WASP-Vrp1 complex act in concert to regulate myoblast fusion in *Drosophila*. All embryos were stained with anti-β3-tubulin. (A-C) Lateral views of stage-16 embryos. (A) Homozygous $scar^{k13811}$ embryos hardly show fusion defects. (B) Unfused myoblasts (arrow) are observed in homozygous $scar^{k13811}$ mutant embryos that lack one copy of $wasp^{3}$. (C) $scar^{k13811}$ $wasp^{3}$ double-mutant embryos display lots of unfused myoblasts (arrow). (D-G) Dorsal views of stage-14/15 embryos. (D) Wild type. (E) Embryos that are homozygous for $scar^{\Delta 37}$ display a weak fusion defect (arrow). Some muscles are missing (arrowhead) and dorsal closure is delayed. (F) $vrp1^{f06715}$ mutant embryos stop fusion after precursor formation. (G) $scar^{\Delta 37}$ $vrp1^{f06715}$ double mutants exhibit a strong myoblast-fusion defect.

Immunostainings of these double mutants with anti-β3-tubulin revealed a dramatically increased myoblast-fusion defect (Fig. 5G) similar to that observed in *Arp3* and *wasp* double mutants.

Taken together, our double-mutant experiments with *scar wasp* and *vrp1* clearly show that *scar* and *wasp* interact genetically during myoblast fusion. Thus, SCAR and the WASP-Vrp1 complex act together during myoblast fusion to regulate the activity of the Arp2/3 complex.

Vrp1 becomes recruited to the tip of filopodia in FCMs, leading to increased F-actin content

To study whether Verprolin is distributed similarly to F-actin during myoblast fusion (Kesper et al., 2007), we generated an anti-Vpr1 antibody and analyzed the subcellular localization of Vrp1 in embryos carrying the rP298 enhancer-trap insertion. The enhancer-trap line rP298 expresses *lacZ* under the control of the Duf regulatory region, and thus marks all nuclei of the FCs and growing muscles (Nose et al., 1998; Ruiz-Gomez et al., 2000). Vrp1 was recently reported to localize to specific foci in FCMs (Kim et al., 2007); however, we observed that this is only the case in FCMs that have not yet formed a filopodia (Fig. 6A′, asterisk). After

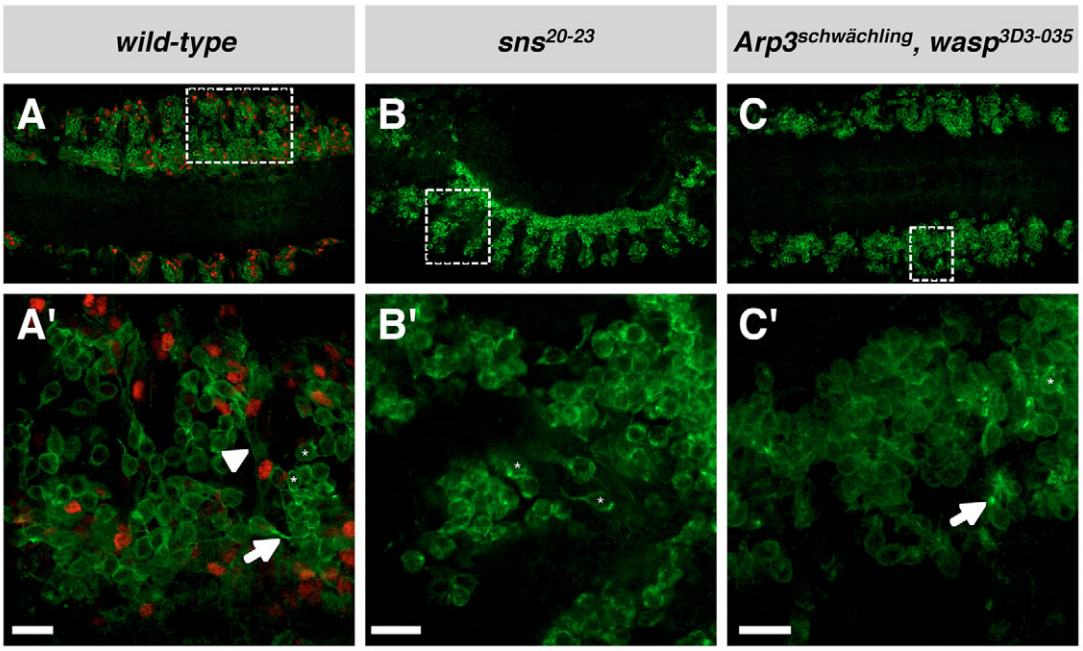

Fig. 6. Vrp1 is expressed in discrete foci, but becomes localized in the filopodia upon cell-cell contact. (A-C) Stage-13/14 embryos stained with anti-Vrp1 antibody. (A′-C′) Higher-magnification views of the boxed areas in A-C. (A) Embryo carrying the enhancer-trap insertion rP298 stained with anti-β-galactosidase and anti-Vrp1. Ventral view of a stage-14 embryo. (A′) In round myoblasts, Vrp1 can be detected in discrete foci (asterisks). However, in FCMs that have formed a filopodium, Vrp1 is enriched at the tip of the FCM, which attaches to a growing myotube (arrow points towards the tip of a filopodium and the arrowhead marks a dinucleated precursor). Note that the precursor cell (arrowhead) also shows a weak expression of Vrp1. (B) sns^{20-23}-null mutant embryo at stage 13; lateral view. (B′) Vrp1 is still present in discrete foci (asterisks); however, no localization of Vrp1 to the tip of a filopodium was observed. (C) Ventral view of a stage-14 $wasp^{3D3-035}$ $Arp3^{schwächling}$ double-mutant embryo. (C′) Vrp1 can be found in round myoblasts in discrete foci (asterisk) and in the tip of a filopodium (arrow). Scale bars: 10 μm.

filopodia formation, however, Vrp1 becomes localized to the tip of the filopodia. In Fig. 6A′, the arrowhead points to a dinucleated myotube in which Vrp1 is faintly expressed. Thus, Vrp1 is concentrated like F-actin at the site of cell-cell contact in FCMs, but not at the site of the FCs. To clarify whether the localization of Vrp1 depends on cell contact, we examined the distribution of Vrp1 in an *sns*-null allele. Although we observed Vrp1 to be still present in $sns^{20\text{-}23}$ (Paululat et al., 1995) embryos, the protein could only be found in discrete foci (Fig. 6B′, asterisks). Accordingly, Vrp1 is restricted to the filopodia of FCMs, in which it attaches to an FC/growing myotube. We therefore assume that Vrp1 increases, together with WASP, the formation of F-actin at the tip of the filopodia. The localization of Vrp1 to the filopodia depends on cell-cell contact, as revealed by immunostainings with anti-Vrp1 on $sns^{20\text{-}23}$ single mutants and on $wasp^{3D3\text{-}035}$ $Arp^{schwächling}$ double mutants (Fig. 6B′ asterisk; Fig.6C′, asterisk and arrow). This further shows that the correct localization of Vrp1 in the double mutant is not disturbed because myoblasts are capable of recognition and adherence. When we applied the anti-Vrp1 antibody to vrp^{f06715} mutant embryos, no staining was detectable, indicating that no protein is generated in $vrp1^{f06715}$ embryos. Taken together, we found that Vrp1 becomes restricted to the filopodia formed by the FCMs after successful cell-cell contact.

FCMs fail to fuse after adhesion

To test whether the initial step of recognition and adhesion between FCs and FCMs is indeed not disturbed in $Arp3^{schwächling}$ and $wasp^{3D3\text{-}035}$ single mutants, or in the double mutants, we investigated the distribution of Duf in those mutants. In wild-type embryos, we observed the typical ring-like structure in which Duf is distributed (Fig. 7A, arrowhead). Furthermore, FCMs could be seen contacting growing muscles (Fig. 7A, asterisk). Fig. 7B shows that, in $Arp3^{schwächling}$ mutants, several FCMs successfully attached to a precursor cell, but did not become integrated into the precursor cell (asterisks). Also, in $wasp^{3D3\text{-}035}$ mutants, FCMs were seen to adhere to a growing myotube (Fig. 7C). These findings are not surprising, because the characterization of the $Arp3^{schwächling}$ and $wasp^{3D3\text{-}035}$ mutant phenotypes has already demonstrated that some fusion takes place in both mutants. However, can FCMs that fail to fuse completely in $Arp3^{schwächling}$ $wasp^{3D3\text{-}035}$ double mutants attach to FCs or is the failure of fusion in the double mutant due to a secondary effect, e.g. cell migration? Fig. 7D shows that FCMs still find their target, thereby suggesting that no secondary effect is involved (asterisks).

Discussion

The genetic data presented in this study provide new insights into the regulation of branching F-actin during myoblast fusion. There are three classes of protein that initiate the polymerization of new actin filaments: the actin-related protein complex Arp2/3, the Formins and Spire. These protein classes are evolutionary conserved in most eukaryotes and promote new actin assembly by a distinct mechanism. The Arp2/3 complex is the only known protein complex that initiates new actin filaments branching off an existing filament. Upon cell-cell contact, F-actin is mostly present in the tip of the FCM and in the area of the FC/growing myotube to which the FCM is attaching (Kesper et al., 2007). Our analyses of *Arp3*, *wasp* and *scar* mutants indicate that branching F-actin is essential for myoblast fusion. Based on our double-mutant analyses, we postulate that the WASP-Vrp1 complex promotes branched F-actin formation positively during the second step of myoblast fusion, thereby allowing us to propose a new model for actin regulation during myoblast fusion (see below).

Cell-cell recognition and adhesion occur normally in mutants in which the actin cytoskeleton machinery is affected

This work emanated from the identification of an *Arp3*-null allele. Fusion is severely disrupted in $Arp3^{schwächling}$ mutants. However, stainings with anti-Duf clearly show that this is not due to a failure in cell-cell recognition and adhesion. For example, FCMs still attach to the site of the growing myotubes where Duf is expressed in $Arp3^{schwächling}$ and $wasp^{3D3\text{-}035}$ mutant embryos. Interestingly, myoblasts also adhere successfully in $Arp3^{schwächling}$ $wasp^{3D3\text{-}035}$ double mutants that fail to fuse completely (compare Fig. 1B and Fig. 4B with Fig. 4C). Duf serves to attract FCMs, which can migrate towards the Duf-expressing source (Ruiz-Gómez et al., 2000). Hence, the ability of FCMs to migrate is a prerequisite for myoblast fusion. The migration of cells, however, also depends on actin-cytoskeleton regulation. Our observations clearly show that the nature of the fusion arrest in $Arp3^{schwächling}$ and $wasp^{3D3\text{-}035}$ single mutants, and $Arp3^{schwächling}$ $wasp^{3D3\text{-}035}$ double mutants, is not due to either the inability of FCMs to migrate nor to a failure of FCs/myotubes and FCMs to recognize and adhere, but rather to a specific defect in cell-cell fusion.

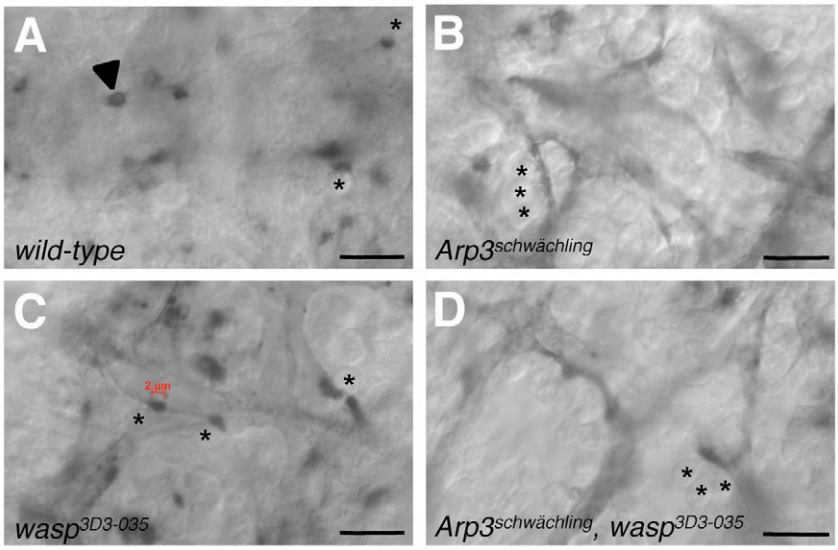

Fig. 7. Duf is localized correctly in $wasp^{3D3\text{-}035}$ and $Arp3^{schwächling}$ mutants, suggesting that assembly of the FuRMAS occurs. (A-D) Anti-Duf staining on stage-15/16 embryos. (A) In a wild-type embryo, Duf is expressed on the site of the FC/growing myotube as a ring (frontal view, arrowhead). The asterisks mark FCMs attaching to a growing myotube (lateral view). (B) Three FCMs attach to a growing myotube (asterisks, lateral view) in an $Arp3^{schwächling}$ embryo. Duf is present on the site of the FC/growing myotube. (C) In a $wasp^{3D3\text{-}035}$ embryo, the asterisks once again highlight FCMs (lateral view) that attach to growing myotubes expressing Duf. (D) In $Arp3^{schwächling}$ $wasp^{3D3\text{-}035}$ double-mutant embryos, Duf is also expressed and concentrated at the site of cell-cell contact. Three FCMs can be seen to attach to a Duf-expressing cell (asterisks). Scale bars: 10 µm.

WASP is required for the creation of an open fusion pore, whereas Arp3 promotes the integration of the FCMs into the growing myotube

Electron microscopy analyses on *Arp3*^{schwächling} and *wasp*$^{3D3\text{-}035}$ mutants further assisted us to dissect the process in which F-actin formation is required during myoblast fusion. The WASP-Vrp1 complex is involved in the formation of a fusion pore, as reported by Massarwa et al. (Massarwa et al., 2007). In line with their study, we observed that mutations in *wasp*$^{3D3\text{-}035}$ and *wip*^{D30} stop fusion during membrane breakdown, but not after pre-fusion-complex formation, as reported by Kim et al. (Kim et al., 2007). We found that the pre-fusion complex, which has been described to consist of 1.4 vesicles per pre-fusion complex (Estrada et al., 2007), looks identical in both of the mutants as well as in wild-type embryos.

Fig. 8A presents a new model for myoblast fusion derived from the data presented in this study, Table 1 summarizes the molecules that are required for the fusion process. Our studies on *Arp3* mutants indicate that the polymerization-based force of branching F-actin is required beyond the stage of membrane breakdown. After

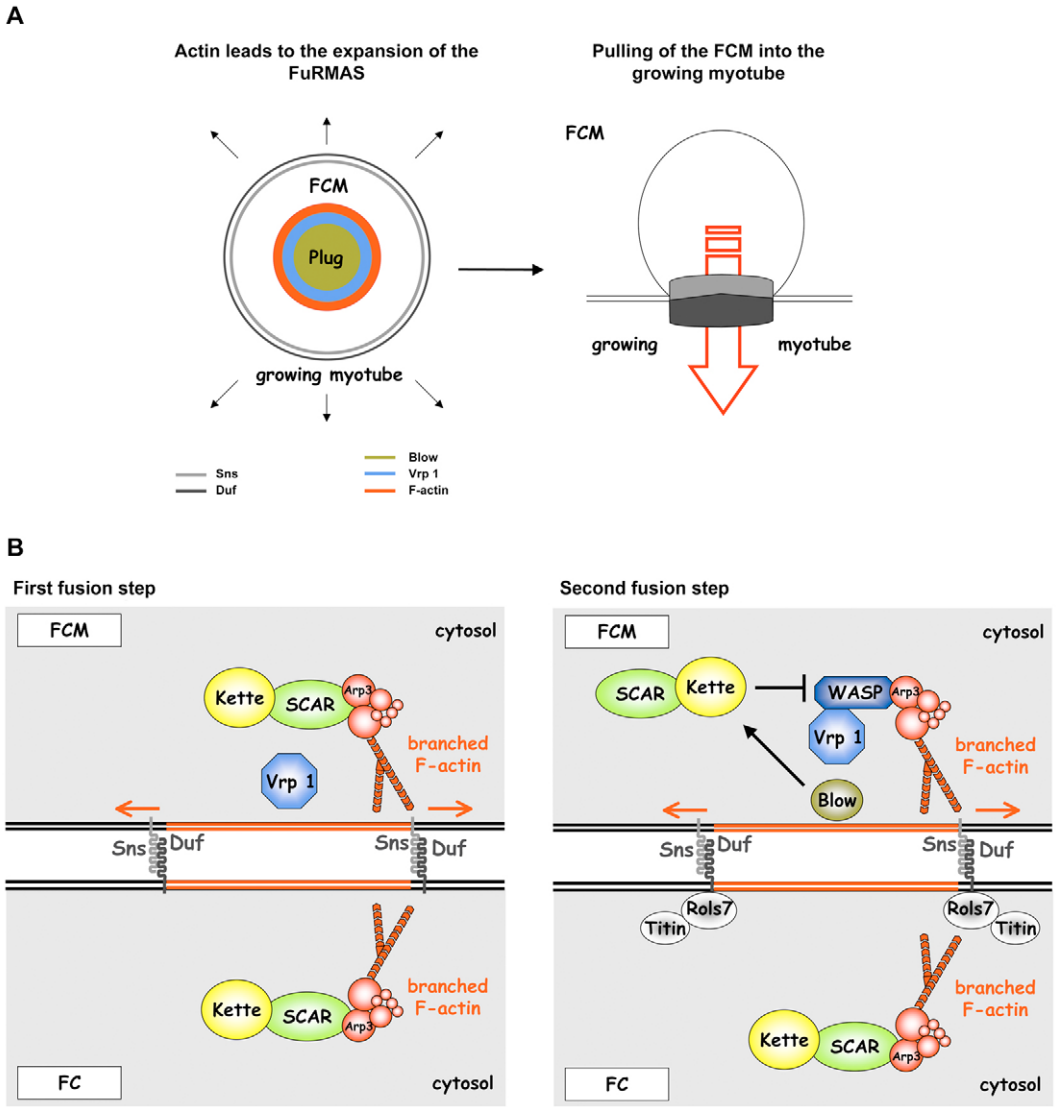

Fig. 8. A modified model for myoblast fusion in *Drosophila*. (A) Actin regulates the expansion of the FuRMAS and integrates the FCM into the growing myotube. Blow is localized to the middle of the ring that expresses Sns in FCMs and Duf in FCs. Our data suggest that Vrp1 is also present in this location, inducing the branching of F-actin in concert with WASP. The correct localization of these components (Kesper et al., 2007) is required for the formation of a fusion pore, and hence their presence guarantees successful fusion. Transmission electron microscopy studies suggest that *wasp* and *vrp1* mutants are capable of forming a pore. In *Arp3* (encoding a subunit of the Arp2/3 complex) mutants, fusion is disrupted after fusion-pore formation. Therefore, we propose that F-actin is required for the integration of FCMs into the FC/growing myotube. (B) Molecular model for regulating F-actin branching during the first and the second step of myoblast fusion. Duf and Sns form a ring in FCs and FCMs, respectively. The fusion pore will be formed in the middle of the ring (indicated in red). We postulate that the SCAR-Kette complex regulates F-actin formation during the first fusion step. The formation of F-actin during the first fusion step might additionally require the activity of Vrp1. During the second fusion step, the signal from the outer membrane in FCs becomes translated by Rols7, which is involved in the localization of *Drosophila* Titin (Menon and Chia, 2001). Our results suggest that F-actin becomes regulated differently in FCs and FCMs. The activity of the actin regulator WASP might be required in FCMs, in which it acts together with Vrp1. We propose that the actin regulators SCAR and Kette are also involved during the second fusion step, because Kette and WASP act antagonistically during the fusion process. Functions of the proteins involved during the first and second fusion step are described in Table 1.

Table 1. Proteins involved in the first and second fusion step of *Drosophila* myoblast fusion

Protein	Function	Localization	Fusion steps
Duf	Mediates cell-adhesion; contains Ig domains	FCs	First and second* (Ruiz-Gomez et al., 2000; Strünkelnberg et al., 2001)
Sns	Mediates cell-adhesion; contains Ig domains	FCMs	First and second (Doberstein et al., 1997; Bour et al., 2000)
Rols7	Multidomain protein required for stabilizing cell adhesion	FCs	Second (Rau et al., 2001)
Kette	F-actin regulation	FCs*, FCMs*	Second* (Schröter et al., 2004)
Blow	F-actin regulation; genetic interactor of kette	FCMs	First and second (Doberstein et al., 1997; Schröter et al., 2004; Beckett and Baylies, 2007)
WASP	F-actin regulation; activates Arp2/3 complex	FCMs*	Second (Schäfer et al., 2007)
Vrp1	F-actin regulation; WASP-interacting partner	FCMs	First and second (this study)
SCAR	F-actin regulation; activates Arp2/3 complex	FCs*, FCMs*	First and second (this study)
Arp3	F-actin formation; subunit of Arp2/3 complex	FCs, FCMs	First and second (this study)
D-Titin	Structural constituent of the actin cytoskeleton	FCs and FCMs	unknown

*, Presumably; D-Titin, *Drosophila* Titin.

membranes have been removed between fusing myoblasts, the FCMs must become integrated into the FC/growing myotube. Because *Arp3*^{schwächling} mutants fail to fuse after membrane removal, we propose that F-actin is required to allow integration into the growing myotubes. After the Duf- and Sns-mediated recognition of FCs and FCMs, further essential proteins for myoblast fusion, e.g. Blow, become recruited to the point of fusion in FCMs. We found that Vrp1 localizes in the tip of the filopodia of FCMs. Kim et al. (Kim et al., 2007) and Massarwa et al. (Massarwa et al., 2007) have shown that the localization of WASP to the membrane depends on Vrp1 activity. Thus, the recruitment of WASP presumably leads to an increase of F-actin at the site of fusion. As a result, the formation of a fusion pore is initiated and expands until the FCM becomes finally pulled into the FC/growing myotube.

The Arp2/3 activators WASP and SCAR control F-actin formation during the second step of myoblast fusion, whereas the first fusion step is independent of WASP

Our morphological and statistical analysis on the nuclei of the DA1 muscle suggested that no fusion takes place in *Arp3 wasp* double mutants. Because *wasp*$^{3D3\text{-}035}$ mutants should lack the ability to promote F-actin formation and stop fusion, like *Arp3*^{schwächling} mutants, after precursor formation, this was a surprising result. We therefore examined whether the actin regulator SCAR additionally controls F-actin branching during myoblast fusion. Double-mutant and epistasis experiments of *scar* and *wasp* revealed that this was indeed the case. The complete disruption of myoblast fusion in *Arp3 wasp* double-mutant embryos – despite the presence of maternal *wasp* and *Arp3* – in conjunction with the finding that SCAR is required for myoblast fusion, led us to propose that SCAR and WASP control different steps of myoblast fusion (Fig. 8B). So far, our genetic data suggest that WASP is only required during the second fusion step. This is in line with previous data presented by Massarwa et al. (Massarwa et al., 2007). It further implies that SCAR is essential for the first fusion step. However, myoblast fusion is not disrupted completely in *scar*$^{\Delta 37}$-null mutant embryos. The maternally provided gene product of *scar* is probably able to compensate for the loss of zygotic *scar* during myoblast fusion. Nevertheless, *scar* germline clones with reduced levels of maternal and zygotic SCAR protein show an enhanced myoblast-fusion phenotype (Richardson et al., 2007). Because the loss of maternal *scar* disrupts oogenesis, it is not possible to eliminate the maternal component of *scar* completely (Zallen et al., 2002). Hence, further experiments are required to determine whether SCAR controls the first fusion step alone or acts in functional redundancy with an additional factor.

Myoblast fusion in *scar vrp1* double mutants was blocked completely. This might indicate that SCAR regulates the first fusion step together with the WASP-interacting partner Vrp1. The Vrp1 protein is expressed from stage 10 onwards, shortly before the first fusion step is initiated. Members of the Verprolin/WIP family have been reported to influence actin polymerization in a WASP-independent manner (reviewed by Anton and Jones, 2006; Aspenström, 2005). It remains to be investigated whether this is also the case during *Drosophila* myoblast fusion.

In addition to regulating the first fusion step, the activity of SCAR might also be required for the second fusion step. Support for this notion comes from our previous findings that the vertebrate homolog of Kette, HEM2, which is present in a complex with SCAR, is essential for myoblast fusion (Schröter et al., 2004). Kette and WASP have antagonistic functions during myoblast fusion (Schäfer et al., 2007). Because we have previously shown that the expression of WASP in FCs failed to rescue the *wasp* mutant phenotype, one could assume that the activity of WASP is only required in FCMs (Schäfer et al., 2007). We therefore predict that the polymerization of branching actin filaments might be regulated in a myoblast-type-specific manner (Fig. 8B).

In summary, our observations suggests for the first time that the cellular machinery leading to the formation of F-actin is controlled by a different set of nucleation-promoting factors during the first and second fusion steps. Future studies should now focus on the mechanistical details to reveal how these factors become activated in FCs and FCMs.

Materials and Methods

Drosophila stocks and genetics

The EMS mutant *Arp3*^{schwächling} was mapped using the deficiency kit from the Bloomington Stock Center. We used the following deficiencies and P-insertions to uncover the *Arp3* gene (breakpoints are indicated): Df(3L)ZP1 (66A17-66C5), Df(3L)pbl-X1 (65F3-66B10), Df(3L)66C-G28 (66B8-66C10) and Arp66B^{EP3640}. We found that Df(3L)66C-G28 is also allelic to *schwächling* and Arp66B^{EP3640}, suggesting that the distal breakpoint of the deficiency (66B8) is not mapped precisely. Oregon R was used as wild-type strain. We used Dr/TM3 Deformed *lacZ* and If/CyO hindgut *lacZ* flies to rebalance our stocks with a blue balancer. Genetic experiments were carried out using the following fly strains: *wasp*^{3}/TM3 (Ben-Yaacov et al., 2001), *wasp*$^{3D3\text{-}035}$/TM3 (Schäfer et al., 2007), *scar*$^{\Delta 37}$/CyO and *scar*^{k13811}/CyO (Zallen et al., 2002). The *vrp1*^{f06715}/CyO strain was ordered from the *Drosophila* Stock Collection at the Harvard Medical School. The *wip*^{D30} allele was obtained from Eyal Schejfer (Weizman Institute, Rehovot, Israel). We used genomic recombination to generate *Arp3*^{schwächling} *wasp*$^{3D3\text{-}035}$, *Arp3*^{schwächling} *wasp*^{3}, *Arp66B*^{EP3640} *wasp*$^{3D3\text{-}035}$ and *scar*$^{\Delta 37}$ *vrp1*^{f06715} double mutants. The rP298 enhancer-trap line (Nose et al., 1998) was used to label founder cells. All crosses were performed at 25°C.

Immunohistochemistry

Embryos were collected on apple-juice plates and aged at 25°C/18°C. Most embryos were fixed as described previously (Hummel et al., 1997). To visualize the muscle pattern, we used the anti-β3-tubulin antibody (Buttgereit et al., 1996; Leiss et al., 1988) at a dilution of 1:12,000 (for DAB staining) and 1:5000 (for fluorescence staining). To distinguish between balancer (*lacZ*)-carrying and homozygous mutant embryos, we additionally used the anti-β-galactosidase antibody (Cappel: 1:5000 dilution). The anti-Eve (3C10: 1:30 dilution) antibody was obtained from the Hybridoma Bank. Anti-Duf stainings (1:1000 dilution) were performed as described previously (Kesper et al., 2007). Cy2- and Cy3-conjugated secondary antibodies were purchased from Dianova. Fluorescent images were acquired using a Leica TCSsp2 confocal scanning microscope.

Whole-mount in situ hybridizations were performed as described previously (Tautz and Pfeifle, 1989). The full-length *Arp3* cDNA LD35711, which was labeled for RNA in situ hybridizations, were obtained from the DGRC.

Antibody generation

Polyclonal antiserum against Vrp1 was generated by injection of guinea pigs with recombinant HIS-tagged protein corresponding to residues 837-936 of Vrp1 in pETM11 (details available upon request). The resulting guinea pig antiserum (Medprobe) was IgG-purifed on a Protein A column (Pierce) prior to use at 1:1000 for immunohistochemistry.

PCRs and sequencing

The insertion of the EP element was confirmed by inverse PCR. We used *Cfo*I to digest the genomic DNA isolated from $Arp66B^{EP3640}$, and Pry1 and Pry2 (BDGP) as primer pairs for inverse PCR. This revealed that the EP-element insertion is located 123 bp in front of the ORF of *Arp3*. To sequence the *Arp3* gene in $Arp3^{schwächling}$ mutants, genomic DNA was isolated from homozygous $Arp3^{schwächling}$ mutant embryos and the coding region of *Arp3* was amplified by PCR. Sequencing was performed by AGOWA (Berlin). For RT-PCR, total RNA was prepared using TRIzol (Invitrogen) from embryos. We used the OneStep RT-PCR Kit (Qiagen) to amplify a 509-bp spliced and a 674-bp unspliced fragment. We used the following primer pairs: forward primer located at the 5′ UTR of LD35711 (5′-CTGGGTTT-ATCTGCAACTG-3′) and reverse primer located within the third exon of LD35711 (3′-GAACGTCTCAAACATTATCTC-5′).

EM analysis

Embryos were fixed in 18% glutaraldehyde:heptan (1:1) for 20 minutes. X-Gal staining was used to detect homozygous mutant embryos that were then devitillinized manually in 0.5% formaldehyde/0.2 M HEPES. Embryos were washed three times in PBS for 10 minutes each, and then the PBS was replaced with 1% OsO_4 and 0.15% ferrisyanide in PBS for 60 minutes. Embryos were washed three times in H_2O for 10 minutes each and incubated with 4% uranylacetate for 60 minutes. Afterwards, embryos were dehydrated in an ethanol series and incubated for 3 hours in Epon (Epoy-embedding kit, Fluka)/Ethanol (1:1). Ultrathin sections were obtained using an Ultracut E microtome (Reichert-Jung) and analyzed with the Hitachi HU-12A electron microscope.

This work was supported by the Deutsche Forschungsgesellschaft (DFG) by the Graduate School 1216 awarded to R.R.-P. and to S.-F.O., as well as by the European Network of Excellence (MYORES). R.H.P. is a Swedish Cancer Foundation Research Fellow supported by the Swedish Research Council (621-2003-3399). We thank Aurelia Fuchs for carrying out the first phenotypic analysis of *scar* mutant embryos. We further thank Sabina Huhn and Helga Kisselbach-Heckmann for technical assistance. The electron microscopy studies were supported by EMBO ASTF 215-2006. The first ultrastructural analysis on wild-type embryos was carried out in collaboration with Andreas Brech in Harald Stenmark's laboratory at the Radium Hospital in Oslo, Norway.

References

Abmayr, S. M., Balagopalan, L., Galletta, B. J. and Hong, S. J. (2005). Myogenesis and muscle development. In *Comprehensive Molecular Insect Science*. Vol. 2 (ed. L.-I. Gilbert, K. Iatrou and S. Gill), pp. 1-45. Oxford: Pergamon.

Anton, I. M. and Jones, G. E. (2006). WIP: a multifunctional protein involved in actin cytoskeleton regulation. *Eur. J. Cell Biol.* **85**, 295-304.

Aspenström, P. (2005). The verprolin family of proteins: regulators of cell morphogenesis and endocytosis. *FEBS Lett.* **579**, 5253-5259.

Bate, M. (1990). The embryonic development of larval muscles in *Drosophila*. *Development* **110**, 791-804.

Baylies, M. K., Bate, M. and Ruiz Gomez, M. (1998). Myogenesis: a view from *Drosophila*. *Cell* **93**, 921-927.

Beckett, K. and Baylies, M. K. (2007). 3D analysis of founder cell and fusion competent myoblast arrangements outlines a new model of myoblast fusion. *Dev. Biol.* **309**, 113-125.

Ben-Yaacov, S., Le Borgne, R., Abramson, I., Schweisguth, F. and Schejter, E. D. (2001). Wasp, the *Drosophila* Wiskott-Aldrich syndrome gene homologue, is required for cell fate decisions mediated by Notch signaling. *J. Cell Biol.* **152**, 1-13.

Bour, B. A., Chakravarti, M., West, J. M. and Abmayr, S. M. (2000). *Drosophila* SNS, a member of the immunoglobulin superfamily that is essential for myoblast fusion. *Genes Dev.* **14**, 1498-1511.

Buttgereit, D., Paululat, A. and Renkawitz-Pohl, R. (1996). Muscle development and attachment to the epidermis is accompanied by expression of beta 3 and beta 1 tubulin isotypes, respectively. *Int. J. Dev. Biol.* **40**, 189-196.

Chen, E. H. and Olson, E. N. (2001). Antisocial, an intracellular adaptor protein, is required for myoblast fusion in *Drosophila*. *Dev. Cell* **1**, 705-715.

Chen, E. H. and Olson, E. N. (2004). Towards a molecular pathway for myoblast fusion in *Drosophila*. *Trends Cell Biol.* **14**, 452-460.

Doberstein, S. K., Fetter, R. D., Mehta, A. Y. and Goodman, C. S. (1997). Genetic analysis of myoblast fusion: blown fuse is required for progression beyond the prefusion complex. *J. Cell Biol.* **136**, 1249-1261.

Estrada, B., Maeland, A. D., Gisselbrecht, S. S., Bloor, J. W., Brown, N. H. and Michelson, A. M. (2007). The MARVEL domain protein, Singles Bar, is required for progression past the pre-fusion complex stage of myoblast fusion. *Dev. Biol.* **307**, 328-339.

Horsley, V. and Pavlath, G. K. (2004). Forming a multinucleated cell: molecules that regulate myoblast fusion. *Cells Tissues Organs* **176**, 67-78.

Hummel, T., Menne, T., Scholz, H., Granderath, S., Giesen, K. and Klambt, C. (1997). CNS midline development in *Drosophila*. *Perspect. Dev. Neurobiol.* **4**, 357-368.

Ibarra, N., Pollitt, A. and Insall, R. H. (2005). Regulation of actin assembly by SCAR/WAVE proteins. *Biochem. Soc. Trans.* **33**, 1243-1246.

Kesper, D. A., Stute, C., Buttgereit, D., Kreiskother, N., Vishnu, S., Fischbach, K. F. and Renkawitz-Pohl, R. (2007). Myoblast fusion in *Drosophila melanogaster* is mediated through a fusion-restricted myogenic-adhesive structure (FuRMAS). *Dev. Dyn.* **236**, 404-415.

Kim, S., Shilagardi, K., Zhang, S., Hong, S. N., Sens, K. L., Bo, J., Gonzalez, G. A. and Chen, E. H. (2007). A critical function for the actin cytoskeleton in targeted exocytosis of prefusion vesicles during myoblast fusion. *Dev. Cell* **12**, 571-586.

Kreisköther, N., Reichert, N., Buttgereit, D., Hertenstein, A., Fischbach, K. F. and Renkawitz-Pohl, R. (2006). *Drosophila* Rolling pebbles colocalises and putatively interacts with alpha-Actinin and the Sls isoform Zormin in the Z-discs of the sarcomere and with Dumbfounded/Kirre, alpha-Actinin and Zormin in the terminal Z-discs. *J. Muscle Res. Cell Motil.* **27**, 93-106.

Leiss, D., Hinz, U., Gasch, A., Mertz, R. and Renkawitz-Pohl, R. (1988). Beta 3 tubulin expression characterizes the differentiating mesodermal germ layer during *Drosophila* embryogenesis. *Development* **104**, 525-531.

Machesky, L. M. and Insall, R. H. (1998). Scar1 and the related Wiskott-Aldrich syndrome protein, WASP, regulate the actin cytoskeleton through the Arp2/3 complex. *Curr. Biol.* **8**, 1347-1356.

Machesky, L. M., Mullins, R. D., Higgs, H. N., Kaiser, D. A., Blanchoin, L., May, R. C., Hall, M. E. and Pollard, T. D. (1999). Scar, a WASp-related protein, activates nucleation of actin filaments by the Arp2/3 complex. *Proc. Natl. Acad. Sci. USA* **96**, 3739-3744.

Massarwa, R., Carmon, S., Shilo, B. Z. and Schejter, E. D. (2007). WIP/WASp-based actin-polymerization machinery is essential for myoblast fusion in Drosophila. *Dev. Cell* **12**, 557-569.

Menon, S. D. and Chia, W. (2001). *Drosophila rolling pebbles*: a multidomain protein required for myoblast fusion that recruits D-Titin in response to the myoblast attractant Dumbfounded. *Dev. Cell* **1**, 691-703.

Miki, H. and Takenawa, T. (1998). Direct binding of the verprolin-homology domain in N-WASP to actin is essential for cytoskeletal reorganization. *Biochem. Biophys. Res. Commun.* **243**, 73-78.

Nose, A., Isshiki, T. and Takeichi, M. (1998). Regional specification of muscle progenitors in *Drosophila*: the role of the *msh* homeobox gene. *Development* **125**, 215-223.

Paululat, A., Burchard, S. and Renkawitz-Pohl, R. (1995). Fusion from myoblasts to myotubes is dependent on the *rolling stone* gene (*rost*) of *Drosophila*. *Development* **121**, 2611-2620.

Rau, A., Buttgereit, D., Holz, A., Fetter, R., Doberstein, S. K., Paululat, A., Staudt, N., Skeath, J., Michelson, A. M. and Renkawitz-Pohl, R. (2001). *rolling pebbles* (*rols*) is required in *Drosophila* muscle precursors for recruitment of myoblasts for fusion. *Development* **128**, 5061-5073.

Richardson, B. E., Beckett, K., Nowak, S. J. and Baylies, M. K. (2007). SCAR/WAVE and ARp2/3 are crucial for cytoskeletal remodeling at the site of myoblast fusion. *Development* **134**, 4357-4367.

Robinson, R. C., Turbedsky, K., Kaiser, D. A., Marchand, J. B., Higgs, H. N., Choe, S. and Pollard, T. D. (2001). Crystal structure of Arp2/3 complex. *Science* **294**, 1679-1684.

Rohatgi, R., Ma, L., Miki, H., Lopez, M., Kirchhausen, T., Takenawa, T. and Kirschner, M. W. (1999). The interaction between N-WASP and the Arp2/3 complex links Cdc42-dependent signals to actin assembly. *Cell* **97**, 221-231.

Ruiz-Gomez, M., Coutts, N., Price, A., Taylor, M. V. and Bate, M. (2000). *Drosophila dumbfounded*: a myoblast attractant essential for fusion. *Cell* **102**, 189-198.

Schäfer, G., Weber, S., Holz, A., Bogdan, S., Schumacher, S., Müller, A., Renkawitz-Pohl, R. and Önel, S. F. (2007). The Wiskott-Aldrich syndrome protein (WASP) is essential for myoblast fusion in Drosophila. *Dev. Biol.* **304**, 664-674.

Schröter, R. H., Lier, S., Holz, A., Bogdan, S., Klämbt, C., Beck, L. and Renkawitz-Pohl, R. (2004). *kette* and *blown fuse* interact genetically during the second fusion step of myogenesis in *Drosophila*. *Development* **131**, 4501-4509.

Schröter, R. H., Buttgereit, D., Beck, L., Holz, A. and Renkawitz-Pohl, R. (2006). Blown fuse regulates morphogenesis but not myoblast fusion of the circular visceral muscles in *Drosophila*. *Differentiation* **74**, 1-14.

Srinivas, B. P., Woo, J., Leong, W. Y. and Roy, S. (2007). A conserved molecular pathway mediates myoblast fusion in insects and vertebrates. *Nat. Genet.* **39**, 781-786.

Strünkelnberg, M., Bonengel, B., Moda, L. M., Hertenstein, A., de Couet, H. G., Ramos, R. G. and Fischbach, K. F. (2001). *rst* and its paralogue *kirre* act redundantly during embryonic muscle development in *Drosophila*. *Development* **128**, 4229-4239.

Takenawa, T. and Miki, H. (2001). WASP and WAVE family proteins: key molecules for rapid rearrangement of cortical actin filaments and cell movement. *J. Cell Sci.* **114**, 1801-1809.

Tautz, D. and Pfeifle, C. (1989). A non-radioactive *in situ* hybridization method for the localization of specific RNAs in *Drosophila* embryos reveals translational control of the segmentation gene *hunchback*. *Chromosoma* **98**, 81-85.

Taylor, M. V. (2000). Muscle development: molecules of myoblast fusion. *Curr. Biol.* **10**, R646-R648.

Taylor, M. V. (2006). Comparison of muscle development in *Drosophila* and vertebrates. In *Muscle Development in Drosophila* (ed. H. Sink), pp. 169-203. New York: Springer, Business Media.

Volkmann, N., Amann, K. J., Stoilova-McPhie, S., Egile, C., Winter, D. C., Hazelwood, L., Heuser, J. E., Li, R., Pollard, T. D. and Hanein, D. (2001). Structure of Arp2/3 complex in its activated state and in actin filament branch junctions. *Science* **293**, 2456-2459.

Zallen, J. A., Cohen, Y., Hudson, A. M., Cooley, L., Wieschaus, E. and Schejter, E. D. (2002). SCAR is a primary regulator of Arp2/3-dependent morphological events in *Drosophila*. *J. Cell Biol.* **156**, 689-701.